

Investigating Particle Size Effects in Catalysis by Applying a Size-Controlled and Surfactant-Free Synthesis of Colloidal Nanoparticles in Alkaline Ethylene Glycol: Case Study of the Oxygen Reduction Reaction on Pt

Jonathan Quinson,^{*,†,∇} Masanori Inaba,^{†,∇} Sarah Neumann,[‡] Andreas A. Swane,[†] J. Bucher,[§] Søren B. Simonsen,^{||} Luise Theil Kuhn,^{||} Jacob J. K. Kirkensgaard,[⊥] Kirsten M. Ø. Jensen,[†] Mehtap Oezaslan,[#] Sebastian Kunz,[‡] and Matthias Arenz^{*,†,§}

[†]Department of Chemistry, University of Copenhagen, Universitetsparken 5, DK-2100 Copenhagen Ø, Denmark

[‡]Institute of Applied and Physical Chemistry, University of Bremen, Leobenerstraße, 28359 Bremen, Germany

[§]Department of Chemistry and Biochemistry, University of Bern, Freiestrasse 3, CH-3012 Bern, Switzerland

^{||}Department of Energy Conversion and Storage, Technical University of Denmark, Frederiksborgvej 399, 4000 Roskilde, Denmark

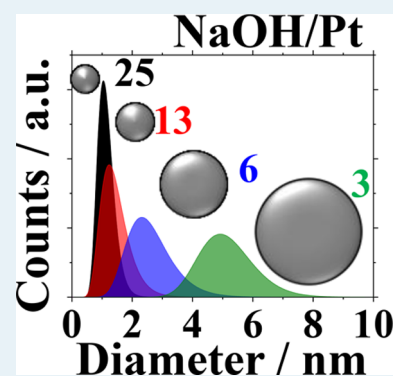
[⊥]Niels Bohr Institute, University of Copenhagen, Universitetsparken 5, 2100 Copenhagen Ø, Denmark

[#]School of Mathematics and Science Department of Chemistry, Carl von Ossietzky Universität Oldenburg, 26111 Oldenburg, Germany

Supporting Information

ABSTRACT: Colloidal platinum nanoparticles are obtained via a surfactant-free polyol process in alkaline ethylene glycol. In this popular synthesis, ethylene glycol functions as solvent and reducing agent. The preparation procedure is known for its reproducibility to obtain 1–2 nm nanoparticles, but at the same time the controlled preparation of larger nanoparticles is challenging. A reliable size control without the use of surfactants is a fundamental yet missing achievement for systematic investigations. In this work it is demonstrated how the molar ratio between NaOH and the platinum precursor determines the final particle size and how this knowledge can be used to prepare and study in a systematic way supported catalysts with defined size and Pt to carbon ratio. Using small-angle X-ray scattering, transmission electron microscopy, infrared spectroscopy, X-ray absorption spectroscopy, pair distribution function, and electrochemical analysis it is shown that when the NaOH/Pt molar ratio is changed from 25 to 3 the Pt nanoparticle size is tuned from 1 to 5 nm. This size range is of interest for various catalytic applications, such as the oxygen reduction reaction (ORR). Supporting the nanoparticles onto a high-surface-area carbon, we demonstrate how the particle size effect can be studied while the Pt to carbon ratio is kept constant, an important aspect that in previous studies could not be accomplished.

KEYWORDS: oxygen reduction reaction, particle size effect, size control, polyol process, platinum nanoparticles, synthesis



INTRODUCTION

Catalysts are essential for many reactions and industrial processes.¹ In particular, precious-metal materials have outstanding catalytic properties for energy conversion or chemical production.^{2–4} To utilize limited resources efficiently, it is key to optimize precious-metal catalysts for specific operation conditions. In many applications, precious-metal catalysts consist of nanoparticles ideally finely distributed on a support material. To optimize the catalytic performance of nanoparticles, one needs to individually investigate and optimize various properties such as the nature of the metal, particle size, support type, metal to support ratio, etc. To best select the most suitable combination of these properties, systematic fundamental research and development of model catalysts must be performed. Since this is a complex multiparameter challenge, a

suitable approach to study and understand the effect of a given property is to control this property independently of the others in a reliable way.

A synthesis method that can address these challenges in the preparation and optimization of precious-metal nanoparticles used as catalysts is based on the “polyol process”.⁵ In the polyol process a metal complex (e.g., H_2PtCl_6) is reduced in an alkaline (e.g., NaOH) solution of a polyol (e.g., ethylene glycol, EG) heated at relatively high temperature (ca. 160 °C). The synthesis recently reviewed⁵ is simple and “green”, which accounts for its popularity and ongoing optimization.⁶ To obtain supported

Received: February 19, 2018

Revised: May 11, 2018

Published: June 6, 2018

nanoparticles, the polyol process is typically performed in a “one-pot” approach, where precious metals are directly formed on a support.⁷ In one-pot syntheses it is often observed that the nature of the support influences the size^{8,9} and the effect of particle size cannot be studied independently of the nature of the support, a severe drawback for systematic studies. In the absence of a support, stable colloidal dispersions of precious-metal nanoparticles can be obtained. Surfactants such as polyvinylpyrrolidone (PVP) or halides are typically used to stabilize the nanoparticles, avoid agglomeration, and tune the particle size.¹⁰ However, these surfactants need to be removed before performing catalytic measurements for optimal catalytic activity.^{11–14} Surfactant removal requires additional steps and treatment of the supported nanoparticles that can potentially influence nanoparticles and support alike, another drawback for systematic studies.

A surfactant-free polyol synthesis has previously been achieved¹⁵ and is known for its high reproducibility for synthesizing 1–2 nm particles. On the basis of this synthesis method we developed a surfactant-free “toolbox” approach of supported catalysts prepared in a two-step synthesis (Figure 1).¹⁶ First, a surfactant-free colloidal dispersion that is stable for

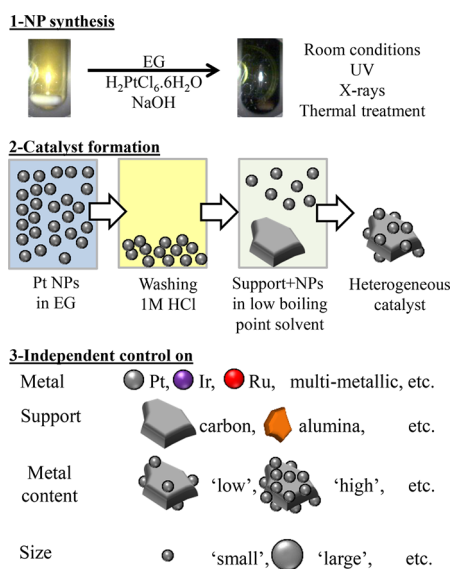


Figure 1. Schematic representation of the steps and ideas to design nanocatalysts by the toolbox approach: (1) surfactant-free colloidal synthesis of Pt nanoparticles (NPs) in alkaline ethylene glycol (EG); (2) Pt nanoparticles supported after acidic washing and redispersion in low-boiling-point solvent; (3) toolbox approach allowing independent control of various experimental parameters for systematic studies and optimization of supported precious-metal catalysts.

months¹⁷ and contains precious-metal nanoparticles is prepared in alkaline EG. The nanoparticles are precipitated by chemical treatment in acid, redispersed, and washed and can then be isolated and stored as a powder¹⁸ or supported by mixing the desired amount of support material and nanoparticles to achieve a target metal to support ratio.^{16,19} A benefit of the two-step approach is that particle formation and growth are independent of the support. The nanoparticles do not form in parts of the support such as pores that are not accessible to the reactants under catalytic operation.²⁰ Thus, the expensive material is more efficiently used during catalysis. Another advantage is that high metal contents (>50 wt %), beneficial to optimize the stability and the mass activity of catalysts,²¹ can be achieved in a single

deposition step. Alternative one-pot syntheses of precious-metal nanoparticles directly on a support material can require multiple iterations of the synthesis before reaching the desired metal content, which leads to undesirable agglomeration of the nanoparticles.²²

The toolbox approach is suitable to understand and study in a systematic way the influence of the various physical catalyst properties such as the nature of the metal, the support, the metal content, the particle size, and the interparticle distance. For this it is essential to be able to change these properties individually, i.e. independent of each other, and to avoid any post-treatment. The toolbox has been successfully exploited to propose routes for improving heterogeneous catalysts in gas sensing,²³ chemical synthesis,^{18,24} and electrocatalysis.^{16,25} For instance, the effects of the carbon support, metal content, and amount of polymer used in “ink” formulation were investigated in a comprehensive way for the oxygen reduction reaction (ORR), which plays a key role in fuel cell development.^{19,21,26} However, a critical missing piece in the toolbox approach was a reliable size control,²⁷ since on the nanoscale the size has a strong influence on catalyst properties such as activity, selectivity, and stability.³

Size control in polyol surfactant-free syntheses can be achieved by changing the viscosity of the solvent. For instance, adding water changes the size,^{15,28} but the obtained colloidal dispersions do not lead in our experience to reproducible results without using a protecting polymer. A general agreement is that pH can be used to affect the size of the nanoparticles, with or without the use of polymer, in colloidal or one-pot syntheses for mono- or bimetallic materials.^{15,17,29–33} It is broadly and commonly stated that the pH must be superior to 12 for the reaction to proceed and that the pH affects the nanoparticle size.

We observed that, when the concentration of platinum precursor is increased, size control is more challenging to achieve. This might explain why, to the best of our knowledge, the concentration of platinum is kept constant in all studies so far, except one³⁴ (see also Table S1). Therefore, controlling the pH (or NaOH concentration) is not sufficient. In the presented work it is demonstrated by using small-angle X-ray scattering (SAXS), transmission electron microscopy (TEM), infrared spectroscopy (FTIR), X-ray absorption spectroscopy (XAS), and pair distribution function (PDF) analysis that it is not the pH which controls the size but the molar ratio between NaOH and platinum. Various samples were prepared with different NaOH/Pt molar ratios using microwave synthesis. It is explained how the nanoparticle size can be tuned in the range 1–5 nm when the NaOH/Pt molar ratio is changed from 25 to 3. Particle dispersions with different sizes are then used to prepare supported Pt/C electrocatalysts with the metal content kept constant and to test the influence of particle size on the oxygen reduction reaction (ORR). In previous work^{35,36} such investigations were possible only by using complex, multistep preparation protocols employing surfactants that typically need to be removed.^{37,38}

RESULTS AND DISCUSSION

NaOH/Pt Molar Ratio To Control Platinum Nanoparticle Size. In previous efforts to achieve size control in surfactant-free colloidal syntheses of precious-metal nanoparticles in alkaline ethylene glycol, pH has been discussed as a crucial parameter.¹⁵ A strict definition of pH is based on the proton activity in aqueous solution. We therefore refrain from using pH and will prefer to use the NaOH concentration. However, it is not always straightforward to reproduce results

from the literature. The concentration of precious-metal precursors in reported studies is typically in the range 0.5–50 mM. The NaOH concentration is typically varied from 0 to 1 M (Table S1). Up to now only the effect of the concentration of the base (NaOH or KOH) has been investigated, with the metal complex concentration kept constant.^{7,39}

The synthesis has recently been performed as a one-pot synthesis including carbon nanotubes as a support material.⁷ No clear correlation between particle size and electrochemically active surface area (ECSA) was found, indicating a profound influence of the support on the obtained catalyst. In particular, the nanoparticle deposition on the support was found to depend on the concentration of NaOH used. The higher the NaOH concentration, the lower the metal content achieved. This is related to the surface charge of the carbon support, leading to repulsive interactions with the nanoparticles. This observation stresses the strong influence of the support on the properties of the prepared catalyst in traditional one-pot syntheses, leading in this specific example to a detrimental effect on the achieved metal content. This drawback is completely alleviated in the toolbox approach, since synthesis and immobilization are independent steps. In another study, in situ SAXS using synchrotron radiation was used to elucidate the temporal evolution of Pt nanoparticle formation in ethylene glycol, with or without surfactant and for different NaOH concentrations, but at a constant H_2PtCl_6 concentration.³⁹ However, synchrotron radiation and X-ray sources (e.g., from an in-house SAXS equipment) are enough in our experience to induce the formation of the nanoparticles (see also the Supporting Information).

In the present study, colloidal platinum nanoparticles were synthesized using a microwave reactor and characterized after synthesis to avoid any support or beam effect during investigation of the nanoparticles. In the microwave reactor based synthesis reactions can be completed in less than 10 min, which enables a high screening output of experimental parameters. The joint influence of the NaOH concentration and the concentration of platinum complex on the resulting size of the platinum nanoparticles is investigated.

TEM and SAXS characterization were carried out on colloidal dispersions of Pt nanoparticles prepared by changing the concentration of NaOH for a given H_2PtCl_6 concentration of 10 mM. Both characterization methods indicate a similar particle size distribution for a given sample; for clarity only the SAXS results are discussed in this first section (Figure 2 and Table S2 and Figure S1). As the concentration of NaOH decreases from 250 to 63 mM, the size of the nanoparticles, evaluated as the mode of the fitted size distribution, increases from 1.1 to 4.9 nm. The trend observed is that, with higher NaOH concentration, the particle size is smaller. This trend agrees with the literature, and it is tempting to conclude that the NaOH concentration controls the size.

The NaOH concentrations used translate to a change in the NaOH/Pt molar ratio from 25 to 3.1. To understand the role of the absolute NaOH concentration in comparison to the NaOH/Pt molar ratio, we further investigated the case of fixed NaOH/Pt molar ratio but varying absolute concentrations. For different concentrations of platinum precursor complex, from 2.5 to 20 mM, the NaOH concentration was changed accordingly from 63 to 500 mM to obtain a constant NaOH/Pt molar ratio of 25. As demonstrated in Figure 2b, in this case, the resulting particle size is the same for all experiments: i.e., around 0.9–1.1 nm. The results unambiguously show that the key parameter to control

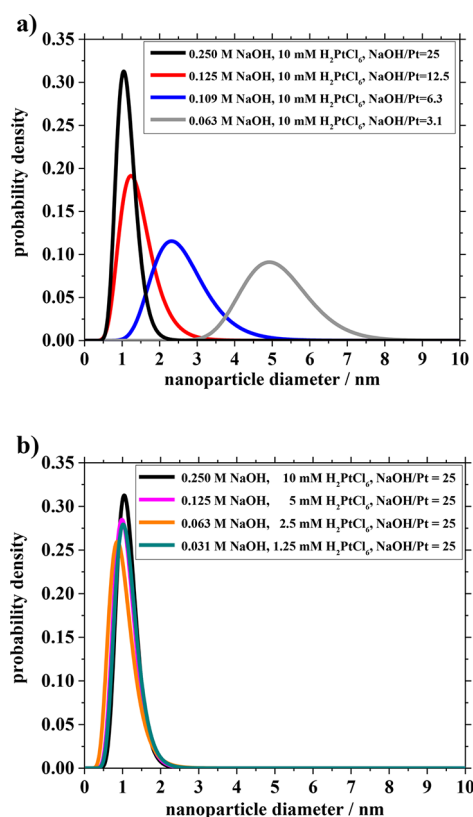


Figure 2. (a) Pt nanoparticle size distribution obtained by SAXS analysis as a function of the concentration of NaOH in the reaction mixture. (b) Pt nanoparticle size distribution obtained by SAXS analysis for different concentrations of NaOH and Pt precursor but the same NaOH/Pt molar ratio of 25. Experimental conditions are detailed in the inset.

the size of the colloidal platinum nanoparticles is the NaOH/Pt molar ratio and not the absolute NaOH concentration. If the NaOH concentration controls the size, the results obtained for 63 mM NaOH with 10 and 2.5 mM H_2PtCl_6 would lead to the same particle size. In contrast, for higher platinum concentration the average particle size is 4.9 nm and that for the lower platinum concentration is 0.9 nm, as demonstrated in our experiments.

The reason for the overlooked assumption in the literature that the pH is key to achieve size control is possibly linked to the pioneering work by Wang et al., who actually investigated the effect of the platinum complex concentration.¹⁵ In their work, no strong effect on the obtained particle size was observed by changing the H_2PtCl_6 concentration from 0.37 to 51 mM. This apparently contradicting statement can be resolved by the fact that they “adjusted the pH” to 12. Since H_2PtCl_6 deprotonates in solution, when higher H_2PtCl_6 concentrations are used, more NaOH is also needed to balance the acidity of the precursor. Therefore, it can be assumed that, in this pioneering work, the authors were unaware that they kept the NaOH/Pt molar ratio close to constant as well. This is why the authors concluded that the method can be used “in a high metal concentration” and lead to narrow size distribution. We scrutinized the size control by the NaOH/Pt molar ratio in two different laboratories (University of Copenhagen and University of Bremen) and for two different preparation methods (oil bath synthesis and microwave reactor) and found reproducible results showing that the NaOH/Pt molar ratio is a more suitable descriptor than absolute NaOH concentration for size control and is more

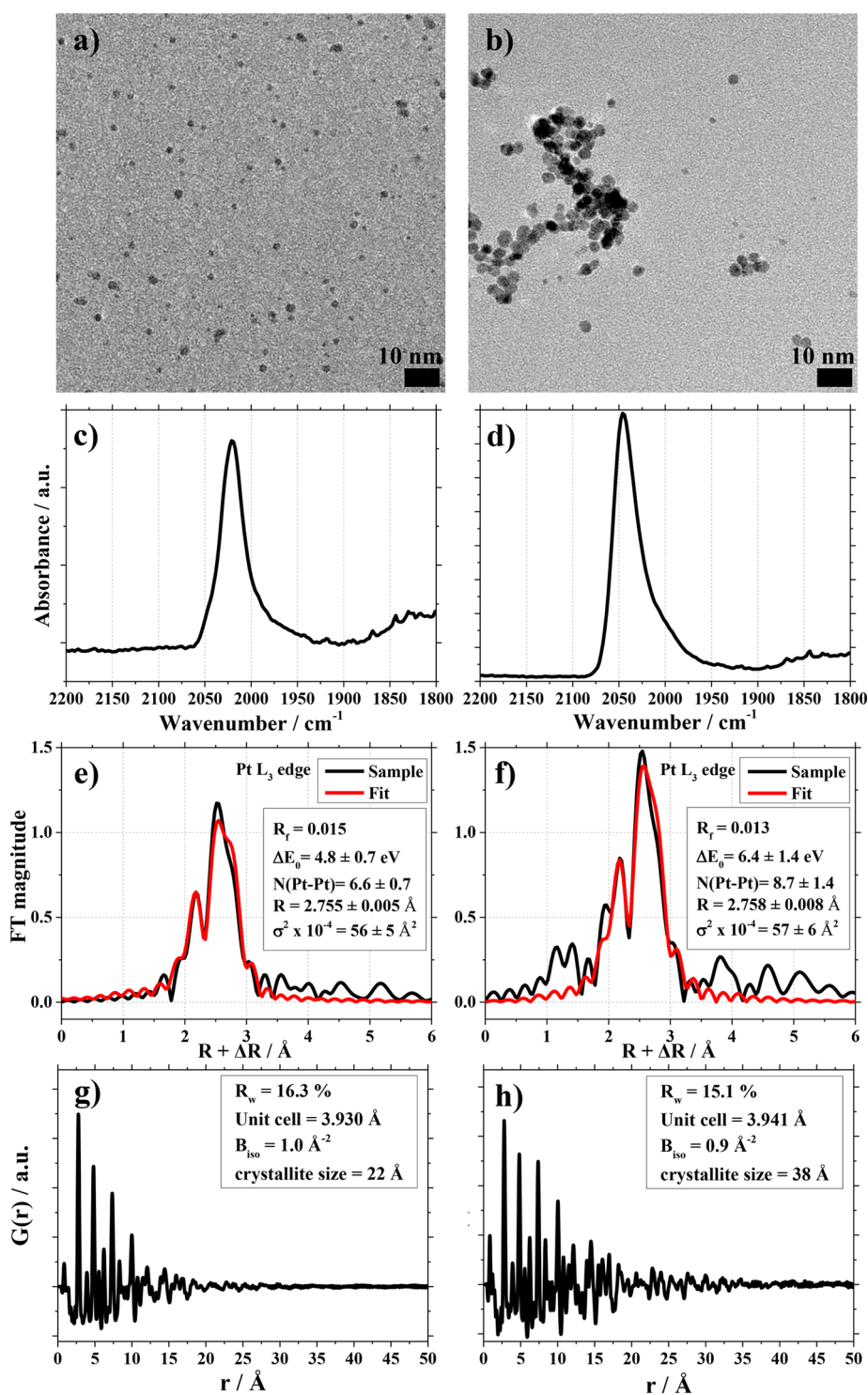


Figure 3. (a, b) TEM, (c, d) FTIR, (e, f) EXAFS for the Pt L₃ edge, and (g, h) PDF characterization of Pt nanoparticles prepared with NaOH/Pt molar ratios of (a, c, e, g) 10 and (b, d, f, h) 4.5.

suitable than pH, with little meaning in nonaqueous solvent. A possible model to account for this observation is outlined in the [Supporting Information](#). In short, estimating the amount of OH⁻ per Pt surface area of the nanoparticles leads to a similar value for each obtained particle size. Therefore, it can be hypothesized that the ratio of OH⁻ to Pt surface atoms not only stabilizes the particles in suspension but also controls the particle growth. As a result, the particle size, or more specifically the

number of Pt surface atoms of a nanoparticle, depends on the chosen NaOH/Pt ratio.

Physical Characterization of Nanoparticles with Different Sizes. A summary of the characterization of as-prepared colloidal Pt nanoparticles obtained with NaOH/Pt molar ratios of 10 and 4.5 by TEM, FTIR, XAS, and PDF analysis is given in [Figure 3](#) and [Table S3](#).

On the basis of the TEM analysis, the nanoparticles obtained with a NaOH/Pt molar ratio of 10 exhibit a mean diameter of

around 2 nm, whereas a NaOH/Pt molar ratio of 4.5 results in diameter in the range 3–5 nm. The TEM data also give indirect evidence of the OH/OH⁻ stabilization: the “unprotected nanoparticles” with a larger size exhibit more agglomeration on the TEM grid in comparison to the smaller nanoparticles as the surface charge from the OH⁻ groups protecting them from agglomeration²⁷ is roughly equal, but larger (heavier) particles need more charge for their stabilization. FTIR characterization reveals absorption bands at 2020 and 2045 cm⁻¹ for the smaller and larger nanoparticles, respectively, attributed to CO surface groups on the Pt nanoparticles.²⁷ The shift to larger wave-number observed for larger nanoparticles is consistent with previous reports^{17,27} and indicates an increase in CO–CO dipole coupling related to the change in the surface curvature of the particles. X-ray absorption near edge structure (XANES) was used to evaluate the degree of oxidation of the Pt in the colloidal suspension, and extended X-ray absorption fine structure (EXAFS) was used to evaluate the average coordination number and bond distance. It is found that, while the initial precursor exists in the form of Pt(IV), after synthesis mainly Pt(0) is detected. On the basis of Fourier-transformed EXAFS data at the Pt L₃ edge, the nanoparticles appear as metallic Pt, suggesting the entire reduction of the Pt(IV) precursor salt after the synthesis. The EXAFS analysis reveals that the atomic length of Pt–Pt bonds is around 2.75 Å, whereas the coordination numbers in the first shell are around 6.6 ± 0.7 and 8.7 ± 1.4 for the nanoparticles prepared with NaOH/Pt molar ratios of 10 and 4.5, respectively. From this analysis, only a rough size estimation can be obtained, but coordination numbers of 6.6 and 8.7 are in agreement with particle sizes of ca. 2 and 3–5 nm, respectively.^{40,41} PDF analysis (see also Figures S3 and S4) is a characterization method well-suited to evaluate the atomic structure and the size of crystal domains in nanomaterials.^{42–44} The analysis shows that the Pt *fcc* crystal structure describes the data well for both nanoparticle sizes and evaluates the crystallite sizes to be 2.2 and 3.8 nm for the smaller and larger nanoparticles, respectively. As expected, the refined unit cell parameter is larger for the largest particles.⁴⁵ The PDF results therefore agree well with TEM, SAXS, and XAS data.

Electrochemical Characterization of Carbon-Supported Pt Nanoparticles with Different Sizes. Among the many applications of platinum nanoparticles in heterogeneous catalysis, a surfactant-free synthesis is especially well-suited for electrocatalysis that requires “clean” catalytic surfaces to ensure efficient electron transfer from/to the catalyst to/from the reactant. One of the main applications of the “toolbox” approach is therefore the preparation of surfactant-free Pt nanoparticles supported on carbon support (Pt/C) catalysts.⁴⁶ The electrochemical properties of carbon-supported Pt/C catalysts prepared with a nominal Pt content of 50 wt % and Pt nanoparticles of different size are summarized in Figure 4 and Table 1. In the cyclic voltammograms (CVs) of all Pt/C catalysts, the typical features of platinum are observed: i.e. the are CVs divided into three main regions, the hydrogen underpotential deposition (H_{upd}) region between 0.05 and 0.35 V (all voltages are expressed versus the reversible hydrogen electrode, RHE), the “double layer” potential region between 0.35 and 0.7 V, where mainly capacitive processes take place, and the “oxide region” above 0.7 V, where OH adsorption and oxide formation on the Pt surface occur.

The CVs of the Pt/C catalysts prepared from the different colloids exhibit an increase in the observed H_{upd} area with

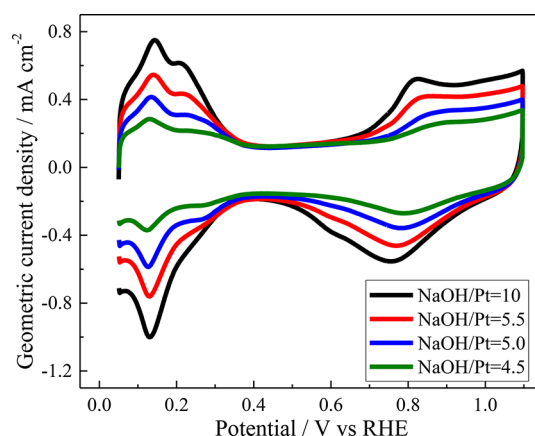


Figure 4. CVs for Pt/C catalysts prepared from different colloidal Pt particle suspensions. The Pt to carbon ratio in the catalyst and the amount of Pt on the glassy carbon were kept constant at 50 wt % and 14 $\mu\text{g}_{\text{Pt}} \text{cm}^{-2}$, respectively. The measurements were conducted in Ar-saturated 0.1 M HClO₄ at a scan rate of 50 mV s⁻¹.

Table 1. ECSA and ORR Activity Values for Homemade and Commercial Pt Catalysts Supported on Carbon^a

NaOH/Pt	diameter (nm)	ECSA (m ² g ⁻¹ _{Pt})	SA (mA cm ⁻²)	MA (A g ⁻¹ _{Pt})
TKK	2.2 ± 0.6	93 ± 7	0.74 ± 0.07	680 ± 70
10	2.1 ± 0.6	102 ± 8	0.90 ± 0.18	922 ± 223
5.5	2.9 ± 0.9	84 ± 2	0.92 ± 0.06	778 ± 37
5	4.0 ± 1.2	54 ± 3	1.06 ± 0.08	570 ± 10
4.5	5.5 ± 1.6	38 ± 1	1.20 ± 0.19	457 ± 52

^aAbbreviations: ECSA, electrochemically active surface area; SA, specific activity @ 0.9 V; MA, mass activity @ 0.9 V. All Pt/C catalysts are prepared with a nominal Pt loading of 50 wt %. ECSA, SA, and MA were evaluated from at least three independent experiments and calculated with respect to the actual Pt content. The particle diameter is estimated by TEM analysis.

increasing NaOH/Pt molar ratio during synthesis. Because the same Pt loading on the GC tip was used for each CV, the observed trend shows that the electrochemical active surface area (ECSA) increases with increasing NaOH/Pt molar ratio. As the ECSA and particle size are correlated with each other, this is expected. The NaOH/Pt molar ratio ultimately influences the electrochemical properties of the nanoparticles. This is also seen by the shift in the peak potential of the oxide reduction peak around 0.8 V. A higher NaOH/Pt molar ratio, and thus smaller Pt particle size, leads to a shift of the oxide reduction peak to lower potentials and can be explained by the higher oxophilicity of smaller Pt nanoparticles.⁴⁷ This is in agreement with ORR tests summarized in Table 1 (see also Figures S5–S8).

It is worth pointing out that several reports using a one-step synthesis of carbon-supported Pt nanoparticles stress the influence of the pH on the maximum metal content achieved.^{7,48,49} As demonstrated, using the presented synthesis approach, the Pt to carbon ratio in the catalyst and the Pt size are controlled independently and the particle size effect^{35,36,50} can be investigated at constant Pt content in the catalyst. When the Pt to carbon support ratio is kept constant but the particle size is varied, a clear trend in electrochemical surface area (ECSA), specific activity (SA), and mass activity (MA) is observed: with increasing particle size, the SA slightly increases, but the ECSA decreases more significantly, resulting in an overall decrease in MA. This study confirms the particle size effect on the ORR

discussed in previous reports: i.e., that the SA increases with particle size. Here, for the first time the metal content in the catalyst is kept constant, and only the particle size is varied. Previous studies changed the particle size and metal content at the same time.^{35,36,50} Our results indicate that initially reported relatively low SA values at very small particle size (or very high ECSA) in the work of Gasteiger et al.³⁶ might be related to the use of relatively low metal to carbon ratio and resulting higher capacitive current contributions. Low metal to carbon ratio to achieve high ECSA values is a direct consequence of practical limitations in the catalyst preparation that are overcome in the approach presented. Thus, the significance of the particle size effect for the ORR was previously overestimated. Changing the particle size from 2 nm to more than 5 nm at constant metal loading increases the SA by less than 50% and is therefore clearly overcompensated by the concurrent significant increase in ECSA.

In addition, the MA obtained with our homemade catalysts is ca. 37% higher than that for a commercial catalyst (TKK) with a similar nanoparticle size (2 nm) and loading (ca. 50 wt %). This can be attributed to the improved control over catalyst optimization using the presented toolbox approach. Our results therefore highlight the benefits of the approach to study and optimize supported catalysts.

CONCLUSIONS

A straightforward control over the size of Pt nanoparticles prepared via the popular alkaline polyol method is achieved by varying the NaOH/Pt molar ratio used during the synthesis. Nanoparticles with controlled size in the range 1–5 nm were successfully obtained using NaOH/Pt ratios between 25 and 3 and characterized by TEM, SAXS, XAS, FTIR, and PDF as well as electrochemical measurements. The characterization confirms that not the pH but the NaOH/Pt molar ratio controls particle size and thus the properties of the as-prepared catalysts. We hypothesize that the concentration of surface species (in our case OH/OH⁻) controls not only the stabilization but also the end of the growth process. The presented finding is an important addition to the toolbox approach, since all fundamental properties of supported catalysts, i.e. particle size, metal loading, support type, etc., can now be independently controlled and tuned for specific applications. In particular, it is demonstrated how the specific activity, electrochemical active surface area, and mass activity of the ORR are influenced by the particle size of Pt at constant metal loading. In comparison to previous investigations,^{35,36,50} the significance of the particle size effect on the ORR is significantly smaller in the present study, which can be explained by the fact that previously catalysts with different Pt loadings were compared: i.e., multiple parameters were changed at the same time.

EXPERIMENTAL SECTION

Polyol Synthesis. For the synthesis of the nanoparticles the polyol synthesis was used.^{15,51–53} The general procedure for a microwave reactor synthesis is detailed.

To obtain ca. 2 nm Pt nanoparticles, 4 mL of a solution of NaOH (98.9%, Fisher Chemical) at 0.4 M in ethylene glycol (EG, 99.8%, Sigma-Aldrich) with an equal volume of a solution of the Pt salt H₂PtCl₆·6H₂O (99.9% Alfa Aesar) at 40 mM in EG was placed in a microwave reaction vessel. The NaOH/Pt molar ratio is then 10 for a H₂PtCl₆ concentration of 20 mM in 8 mL.

The mixture was heated for 3 min at 160 °C with a microwave reactor (CEM Discover SP) using a power of 100 W.

To obtain ca. 4 nm Pt nanoparticles, 4 mL of a solution of NaOH at 90 mM in EG with an equal volume of a solution of the Pt salt H₂PtCl₆·6H₂O at 20 mM in EG was placed in a microwave reaction vessel. The NaOH/Pt ratio is then 4.5 for a H₂PtCl₆ concentration of 10 mM in 8 mL. The mixture was heated for 3 min at 160 °C.

Unless otherwise specified in the figure captions, the nanoparticles were obtained following the general procedure: 20 mM H₂PtCl₆ in 8 mL of alkaline EG for a synthesis time of 3 min at 160 °C and for various NaOH/Pt molar ratios.

The general procedure to obtain nanoparticles with the oil bath synthesis was to carry out the reaction using an organic oil bath preheated to 160 °C. The Pt and NaOH solutions were then placed in a round-bottomed flask and submerged with stirring in the oil bath. After approximately 5 min, the solution turned dark, as in the microwave synthesis, and the colloidal suspension was heated for another 85 min to ensure that all the Pt had been reduced.

Pt Nanoparticle Washing and Immobilization on Carbon. To collect the particles, an aqueous solution (Milli-Q, Millipore, 18.2 MΩ cm) of ca. 30 mL of 1 M HCl (prepared from 30% HCl Suprapur, EMD Millipore, Merck KGaA) was added to 7.3 mL of the Pt nanoparticles in EG. The mixture was centrifuged at 2400g relative centrifugal force (4000 rotations per minute, Sigma 2-5) for 5 min. The nanoparticles could then be collected, since they were no longer a stable colloidal dispersion. The washing/centrifugation with 1 M HCl in Milli-Q water was performed three times. The nanoparticles were redispersed in 7 mL of acetone (technical grade), and a desired mass of carbon black was added (Vulcan XC72R, Cabot Corporation) so that the Pt/C ratio was equal to 50 wt %. By simply sonicating the mixture with an ultrasonic bath (VWR ultrasonic cleaner) for 1 h, the acetone evaporated and a dried powder of Pt nanoparticles supported on carbon was obtained. The powder was redispersed into water and the dispersion sonicated for 10 min. The powder was then filtered and washed with Milli-Q water.

The obtained Pt/C ratio was controlled by an indirect Pt proof (IPP). In short, a part of the respective Pt/C sample (typically around 1–2 mg) was weighed and transferred to a glass tube, where the carbon was carefully burned off with a gas burner. To digest the Pt, 0.5 mL of aqua regia (mixture of 37% HCl and 65% HNO₃ in a volume ratio of 1/0.206) was added and heated in a water bath at ca. 60 °C for 2 h. Thereafter, ca. 5–10 mL of deionized (DI) water was added and the pH was adjusted to a value of 6.8–7.0, controlled by a pH meter. Finally, the sample volume was expanded to 25 mL. The Pt concentration was determined by an IPP method, which had been confirmed with Pt calibration solutions and by comparison to commercial Pt/C samples as well as standard ICP-MS analysis. For the IPP method, a spatula of copper powder and a small piece of the Pt bulk material were added to the prepared aqua regia sample and stirred for 10 min at room temperature. Thereafter the solution was filtered to separate the solids from the liquids and 1 mL of the filtrate was mixed with 2 mL of DI water and two drops of 0.25 M HCl as well as a spatula of a Murexid/NaCl mixture. Finally, the pH was adjusted to 8–10 by adding 1 M NH₃ (the color should change to yellow) and the prepared sample was titrated against 0.1 mM ethylenediaminetetraacetic acid (EDTA). For each sample 10 titrations were performed to give a reliable average.

SAXS Characterization. The as-prepared colloidal suspensions were placed in quartz capillaries for SAXS measurements. The measurements and subsequent modeling to extract particle size distribution were performed as previously described^{16,19,27} and detailed in the [Supporting Information](#) using a SAXSLab instrument installed at the Niels Bohr Institute of the University of Copenhagen.

TEM Characterization. For TEM analysis of the as-produced colloidal solution a JEOL 2100 microscope operated at 200 kV was used. To characterize the supported catalyst on carbon, a FEI Tecnai Spirit microscope operated at 80 kV was used. The size analysis was performed by measuring the size of typically 300 (at least 180) nanoparticles and samples characterized by taking images of (at least) three different magnifications in (at least) five different areas of the TEM grids. The TEM grids were prepared by dropping solutions of nanoparticles redispersed in acetone or the ink redispersed in isopropyl alcohol/Milli-Q water (1/3, v/v) on carbon support films on Cu 300 mesh grids (Quantifoil). ImageJ software was used to measure the nanoparticle sizes, and the nanoparticles were counted manually (without automated processing of the image). For each sample obtained under different experimental conditions, the mean value of the particle size was used to estimate the average diameter of the nanoparticles; the deviations reported correspond to the standard deviation.

FTIR Characterization. The as-synthesized colloidal dispersions in alkaline EG were placed in a cell that allowed the recording of IR spectra of liquid sample in an attenuated total reflectance mode by FTIR spectroscopy. Infrared spectra were captured using a Nicolet 6700 FT-IR instrument (Thermo Electron Corporation) with a zinc selenite prism. All spectra were recorded with a resolution of 4 cm⁻¹ and averaged over 100 scans. A background spectrum of EG was measured and subtracted from the spectra recorded for the colloidal suspension. Only the difference spectra are reported.

XAS (EXAFS/XANES). XAS measurements were performed at the B18 beamline at the Diamond Light Source (DLS), Harwell, U.K. The storage ring of the DLS was operated at beam currents of 300 and 400 mA, respectively, and the storage ring energies were 3.0 and 2.4 GeV, respectively. The Pt L₃ edge XAS spectra were recorded in fluorescence mode by using a nine-element Ge solid-state detector system. The averaged XAS spectra were then analyzed by using the IFEFFIT software suite.⁵⁴ All spectra were background-subtracted and normalized. The energy units (eV) were converted to photoelectron wave vector k units (Å⁻¹) by assigning the photoelectron energy origin, E_0 , corresponding to $k = 0$, to the first inflection point of the absorption edge. The resulting $\chi(k)$ functions were weighted with k^2 to compensate for the dampening of the XAFS amplitude with increasing k . The resulting EXAFS spectra then were Fourier-transformed to obtain pseudo radial structure functions (RSFs).

To estimate the amplitude reduction factor (S_0^2), a Pt foil was used as reference. The coordination number (N), interatomic bond length (R), mean squared bond length disorder (σ^2), and correction to the energy origin (ΔE_0), together with their error bars, were established for each sample by fitting theoretical EXAFS signals to the data in r space. The R_f factor reported indicates the closeness of the fit to the data as a quality parameter. The linear fit combination method was carried out to establish the oxidation of Pt ions in the liquid by using the respective XANES spectra from K₂PtCl₄ (99.9% Alfa Aesar), K₂PtCl₆ (99.9% Alfa Aesar), and Pt foil.

The samples used were characterized as synthesized and after washing with HCl before redispersion in EG. No strong differences could be observed between the samples before or after washing.

PDF Characterization. X-ray total scattering data were collected at beamline P02.1, PETRAIII, DESY using an X-ray wavelength of 0.2072 Å and a PerkinElmer amorphous silicon detector (40 × 40 cm) at a detector distance of 20.059 cm. The samples were loaded in 1 mm Kapton tubes. Data were collected for each sample for 12 min. The nanoparticles were washed in HCl as described above and redispersed in ethylene glycol (concentration of 2 mM) for the measurements. Ethylene glycol was used as background. The data were integrated using Fit2D⁵⁵ and Fourier transformed in the xPDF suite.⁵⁶ To extract quantitative information, the PDFs were modeled using Diffpy-CMI.⁵⁷ The PDFs were modeled applying the *fcc* structure (space group *Fd3m*) and a spherical dampening function, describing the crystallite size. The data analysis is described further in the [Supporting Information](#).

Electrochemical Characterization. The electrochemical measurements were performed using a home-built potentiostat and a rotating disk electrode (RDE) setup. The electrochemical cell was a home-built Teflon cell based on a three-compartment configuration. Platinum mesh and a saturated calomel electrode (Schott) were used as a counter electrode and a reference electrode, respectively. All potentials in this work are referred to the reversible hydrogen electrode (RHE) potential, which was experimentally determined for each measurement series. HClO₄ (0.1 M) was prepared as the electrolyte with 70% HClO₄ (Merck, suprapur) and Milli-Q water.

Prior to the RDE measurements, a glassy-carbon (GC) disk electrode (5 mm in diameter) was polished to a mirror finish using 0.3 and 0.05 μm alumina oxide paste (Struers, AP-D and AP-A suspension) and cleaned ultrasonically in Milli-Q water. Catalyst ink was prepared by mixing typically 5.5 mg of catalyst powder with 7.5 mL of Milli-Q water and 2.5 mL of isopropyl alcohol (IPA, 99.7+ %, Alfa Aesar). A few microliters of 1 M KOH solution was also added to the ink so that the pH of the ink was between 10 and 11. The glass vial containing catalyst ink was sonicated for 15 min. A 10 μL aliquot of the ink was pipetted onto the GC electrode, leading to a Pt loading of 14 μg_{Pt} cm⁻², and thereafter dried under an IPA atmosphere at room temperature.⁵¹

All electrochemical measurements were performed in 0.1 M HClO₄ solution at 20 °C. The solution resistance between the working electrode and the Luggin capillary was determined using an ac signal (5 kHz, 5 mV) and thereafter compensated for using the potentiostat's analog positive feedback scheme. The resulting effective solution resistance was less than 3 Ω for each experiment. Prior to the measurements the electrolyte was deaerated by purging with Ar gas (99.998%, Air Liquide), and the measurements were started with cleaning of the catalyst by potential cycles between 0.05 and 1.2 V at a scan rate of 500 mV s⁻¹.

The electrochemical surface area (ECSA) of the catalyst was determined from CO stripping charge recorded at a scan rate of 50 mV s⁻¹ and a conversion coefficient of 396 μC cm⁻². The catalytic activity for the oxygen reduction reaction (ORR) was determined from positive-going polarization curves recorded in O₂-saturated electrolyte at a scan rate of 50 mV s⁻¹ and a rotation speed of 1600 rpm. The polarization curves were corrected for the non-Faradaic background by subtracting the cyclic voltammograms (CVs) recorded in Ar-purged electrolyte.

■ ASSOCIATED CONTENT

● Supporting Information

The Supporting Information is available free of charge on the ACS Publications website at DOI: 10.1021/acscatal.8b00694.

Literature summary on size control in surfactant-free polyol synthesis of platinum nanoparticles, SAXS, characterization of nanoparticles obtained with different NaOH/Pt molar ratio, and PDF, TEM, and electrochemical data (PDF)

■ AUTHOR INFORMATION

Corresponding Authors

*E-mail for J.Q.: jonathan.quinson@chem.ku.dk.

*E-mail for M.A.matthias.arenz@dcb.unibe.ch.

ORCID

Jonathan Quinson: 0000-0002-9374-9330

Søren B. Simonsen: 0000-0001-7172-1225

Jacob J. K. Kirkensgaard: 0000-0001-6265-0314

Matthias Arenz: 0000-0001-9765-4315

Author Contributions

[∇]J.Q. and M.I. contributed equally.

Notes

The authors declare no competing financial interest.

■ ACKNOWLEDGMENTS

M.A. acknowledges the support from the Villum Foundation in form of a block stipend. J.Q. has received funding from the European Union's Horizon 2020 research and innovation program under the Marie Skłodowska-Curie grant agreement No 703366 (SELECTRON). M.I. acknowledges the support of Toyota Central R&D Laboratories, Inc. K.M.Ø.J. acknowledges funding from the Danish Research Council under the Sapere Aude research Talent Program. Diamond Light Source, Harwell, U.K., is thanked—in particular Dr. Giannantonio Cibin and Ann-Kathrin Geiger—for access to synchrotron beamline B18 (proposal SP12746) that contributed to the results presented. We acknowledge beamtime granted at beamline P02.1, PETRAIII, DESY, a member of the Helmholtz Association (HGF). We thank Martin Etter for assistance in the PDF measurements. S.K. gratefully acknowledges the “Fonds der Chemischen Industrie” (FCI) for financial support through a Liebig Research Grant.

■ REFERENCES

- (1) Oliveira, S.; Forster, S. P.; Seeger, S. Nanocatalysis: Academic Discipline and Industrial Realities. *J. Nanotechnol.* **2014**, *2014*, 324089.
- (2) Rai, M.; Ingle, A. P.; Birla, S.; Yadav, A.; Dos Santos, C. A. Strategic Role of Selected Noble Metal Nanoparticles in Medicine. *Crit. Rev. Microbiol.* **2016**, *42*, 696–719.
- (3) Antolini, E. Structural Parameters of Supported Fuel Cell Catalysts: The Effect of Particle Size, Inter-Particle Distance and Metal Loading on Catalytic Activity and Fuel Cell Performance. *Appl. Catal., B* **2016**, *181*, 298–313.
- (4) Chen, C. W.; Tano, D.; Akashi, M. Colloidal Platinum Nanoparticles Stabilized by Vinyl Polymers with Amide Side Chains: Dispersion Stability and Catalytic Activity in Aqueous Electrolyte Solutions. *J. Colloid Interface Sci.* **2000**, *225*, 349–358.
- (5) Dong, H.; Chen, Y. C.; Feldmann, C. Polyol Synthesis of Nanoparticles: Status and Options Regarding Metals, Oxides, Chalcogenides, and Non-Metal Elements. *Green Chem.* **2015**, *17*, 4107–4132.
- (6) Alekseenko, A. A.; Ashihina, E. A.; Shpanko, S. P.; Volochaev, V. A.; Safronenko, O. I.; Guterman, V. E. Application of CO Atmosphere in the Liquid Phase Synthesis as a Universal Way to Control the Microstructure and Electrochemical Performance of Pt/C Electro-catalysts. *Appl. Catal., B* **2018**, *226*, 608–615.
- (7) Aoun, N.; Schlange, A.; dos Santos, A. R.; Kunz, U.; Turek, T. Effect of the OH-/Pt Ratio During Polyol Synthesis on Metal Loading and Particle Size in DMFC Catalysts. *Electrocatalysis* **2016**, *7*, 13–21.
- (8) Liu, J.; Liu, C. T.; Zhao, L.; Zhang, J. J.; Zhang, L. M.; Wang, Z. B. Effect of Different Structures of Carbon Supports for Cathode Catalyst on Performance of Direct Methanol Fuel Cell. *Int. J. Hydrogen Energy* **2016**, *41*, 1859–1870.
- (9) Qin, Y. H.; Yang, H. H.; Zhang, X. S.; Li, P.; Ma, C. A. Effect of Carbon Nanofibers Microstructure on Electrocatalytic Activities of Pd Electrocatalysts for Ethanol Oxidation in Alkaline Medium. *Int. J. Hydrogen Energy* **2010**, *35*, 7667–7674.
- (10) Cookson, J. The Preparation of Palladium Nanoparticles. *Platinum Met. Rev.* **2012**, *56*, 83–98.
- (11) Park, J. Y.; Aliaga, C.; Renzas, J. R.; Lee, H.; Somorjai, G. A. The Role of Organic Capping Layers of Platinum Nanoparticles in Catalytic Activity of CO Oxidation. *Catal. Lett.* **2009**, *129*, 1–6.
- (12) Naresh, N.; Wasim, F. G. S.; Ladewig, B. P.; Neergat, M. Removal of Surfactant and Capping Agent from Pd Nanocubes (Pd-NCs) Using Tert-butylamine: its Effect on Electrochemical Characteristics. *J. Mater. Chem. A* **2013**, *1*, 8553–8559.
- (13) Safo, I. A.; Oezaslan, M. Electrochemical Cleaning of Polyvinylpyrrolidone-capped Pt Nanocubes for the Oxygen Reduction Reaction. *Electrochim. Acta* **2017**, *241*, 544–552.
- (14) Li, D. G.; Wang, C.; Tripkovic, D.; Sun, S. H.; Markovic, N. M.; Stamenkovic, V. R. Surfactant Removal for Colloidal Nanoparticles from Solution Synthesis: The Effect on Catalytic Performance. *ACS Catal.* **2012**, *2*, 1358–1362.
- (15) Wang, Y.; Ren, J. W.; Deng, K.; Gui, L. L.; Tang, Y. Q. Preparation of Tractable Platinum, Rhodium, and Ruthenium Nanoclusters with Small Particle Size in Organic Media. *Chem. Mater.* **2000**, *12*, 1622–1627.
- (16) Speder, J.; Altmann, L.; Roefzaad, M.; Baumer, M.; Kirkensgaard, J. J. K.; Mortensen, K.; Arenz, M. Pt Based PEMFC Catalysts Prepared from Colloidal Particle Suspensions - a Toolbox for Model Studies. *Phys. Chem. Chem. Phys.* **2013**, *15*, 3602–3608.
- (17) Baranova, E. A.; Bock, C.; Ilin, D.; Wang, D.; MacDougall, B. Infrared Spectroscopy on Size-controlled Synthesized Pt-Based Nano-Catalysts. *Surf. Sci.* **2006**, *600*, 3502–3511.
- (18) Neumann, S.; Grotheer, S.; Tielke, J.; Schrader, I.; Quinson, J.; Zana, A.; Oezaslan, M.; Arenz, M.; Kunz, S. Nanoparticles in a Box: a Concept to Isolate, Store and Re-Use Colloidal Surfactant-Free Precious Metal Nanoparticles. *J. Mater. Chem. A* **2017**, *5*, 6140–6145.
- (19) Speder, J.; Altmann, L.; Baumer, M.; Kirkensgaard, J. J. K.; Mortensen, K.; Arenz, M. The Particle Proximity Effect: from Model to High Surface Area Fuel Cell Catalysts. *RSC Adv.* **2014**, *4*, 14971–14978.
- (20) Strobel, R.; Stark, W. J.; Mädler, L.; Pratsinis, S. E.; Baiker, A. Flame-Made Platinum/Alumina: Structural Properties and Catalytic Behaviour in Enantioselective Hydrogenation. *J. Catal.* **2003**, *213*, 296–304.
- (21) Speder, J.; Zana, A.; Spanos, I.; Kirkensgaard, J. J. K.; Mortensen, K.; Hanzlik, M.; Arenz, M. Comparative Degradation Study of Carbon Supported Proton Exchange Membrane Fuel Cell Electrocatalysts - The Influence of the Platinum to Carbon Ratio on the Degradation Rate. *J. Power Sources* **2014**, *261*, 14–22.
- (22) Deutschmann, O.; Knözinger, H.; Kochloeff, K.; Turek, T. Heterogeneous Catalysis and Solid Catalysts. In *Ullmann's Encyclopedia of Industrial Chemistry*; Wiley, 2009.
- (23) Morsbach, E.; Brauns, E.; Kowalik, T.; Lang, W.; Kunz, S.; Baumer, M. Ligand-Stabilized Pt Nanoparticles (NPs) as Novel Materials for Catalytic Gas Sensing: Influence of the Ligand on Important Catalytic Properties. *Phys. Chem. Chem. Phys.* **2014**, *16*, 21243–21251.

- (24) Schrader, I.; Neumann, S.; Himstedt, R.; Zana, A.; Warneke, J.; Kunz, S. The Effect of Particle Size and Ligand Configuration on the Asymmetric Catalytic Properties of Proline-Functionalized Pt-Nanoparticles. *Chem. Commun.* **2015**, *51*, 16221–16224.
- (25) Speder, J.; Zana, A.; Arenz, M. The Colloidal Tool-Box Approach for Fuel Cell Catalysts: Systematic Study of Perfluorosulfonate-Ionomer Impregnation and Pt Loading. *Catal. Today* **2016**, *262*, 82–89.
- (26) Speder, J.; Zana, A.; Spanos, I.; Kirkensgaard, J. J. K.; Mortensen, K.; Arenz, M. On the Influence of the Pt to Carbon Ratio on the Degradation of High Surface Area Carbon Supported PEM Fuel Cell Electrocatalysts. *Electrochem. Commun.* **2013**, *34*, 153–156.
- (27) Schrader, I.; Warneke, J.; Neumann, S.; Grotheer, S.; Swane, A. A.; Kirkensgaard, J. J. K.; Arenz, M.; Kunz, S. Surface Chemistry of "Unprotected" Nanoparticles: A Spectroscopic Investigation on Colloidal Particles. *J. Phys. Chem. C* **2015**, *119*, 17655–17661.
- (28) Wang, Y. J.; Zhao, N. N.; Fang, B. Z.; Li, H.; Bi, X. T. T.; Wang, H. J. Effect of Different Solvent Ratio (Ethylene Glycol/Water) on the Preparation of Pt/C Catalyst and its Activity Toward Oxygen Reduction Reaction. *RSC Adv.* **2015**, *5*, 56570–56577.
- (29) Bock, C.; Paquet, C.; Couillard, M.; Botton, G. A.; MacDougall, B. R. Size-Selected Synthesis of PtRu Nano-Catalysts: Reaction and Size Control Mechanism. *J. Am. Chem. Soc.* **2004**, *126*, 8028–8037.
- (30) Li, X.; Chen, W. X.; Zhao, J.; Xing, W.; Xu, Z. D. Microwave Polyol Synthesis of Pt/CNTs Catalysts: Effects of pH on Particle Size and Electrocatalytic Activity for Methanol Electrooxidation. *Carbon* **2005**, *43*, 2168–2174.
- (31) Qiu, J. S.; Zhang, H. Z.; Liang, C. H.; Li, J. W.; Zhao, Z. B. Co/CNF Catalysts Tailored by Controlling the Deposition of Metal Colloids onto CNFs: Preparation and Catalytic Properties. *Chem. - Eur. J.* **2006**, *12*, 2147–2151.
- (32) Chu, Y. Y.; Wang, Z. B.; Gu, D. M.; Yin, G. P. Performance of Pt/C Catalysts Prepared by Microwave-Assisted Polyol Process for Methanol Electrooxidation. *J. Power Sources* **2010**, *195*, 1799–1804.
- (33) Kawasaki, H.; Kosaka, Y.; Myoujin, Y.; Narushima, T.; Yonezawa, T.; Arakawa, R. Microwave-Assisted Polyol Synthesis of Copper Nanocrystals without Using Additional Protective Agents. *Chem. Commun.* **2011**, *47*, 7740–7742.
- (34) He, B. L.; Chen, Y. X.; Liu, H. F.; Liu, Y. Synthesis of Solvent-Stabilized Colloidal Nanoparticles of Platinum, Rhodium, and Ruthenium by Microwave-Polyol Process. *J. Nanosci. Nanotechnol.* **2005**, *5*, 266–270.
- (35) Mayrhofer, K. J. J.; Blizanac, B. B.; Arenz, M.; Stamenkovic, V. R.; Ross, P. N.; Markovic, N. M. The Impact of Geometric and Surface Electronic Properties of Pt-Catalysts on the Particle Size Effect in Electrocatalysis. *J. Phys. Chem. B* **2005**, *109*, 14433–14440.
- (36) Gasteiger, H. A.; Kocha, S. S.; Sompalli, B.; Wagner, F. T. Activity Benchmarks and Requirements for Pt, Pt-alloy, and non-Pt Oxygen Reduction Catalysts for PEMFCs. *Appl. Catal., B* **2005**, *56*, 9–35.
- (37) Li, D. G.; Wang, C.; Strmcnik, D. S.; Tripkovic, D. V.; Sun, X. L.; Kang, Y. J.; Chi, M. F.; Snyder, J. D.; van der Vliet, D.; Tsai, Y. F.; Stamenkovic, V. R.; Sun, S. H.; Markovic, N. M. Functional Links between Pt Single Crystal Morphology and Nanoparticles with Different Size and Shape: the Oxygen Reduction Reaction Case. *Energy Environ. Sci.* **2014**, *7*, 4061–4069.
- (38) Lv, H. F.; Li, D. G.; Strmcnik, D.; Paulikas, A. P.; Markovic, N. M.; Stamenkovic, V. R. Recent advances in the design of tailored nanomaterials for efficient oxygen reduction reaction. *Nano Energy* **2016**, *29*, 149–165.
- (39) Steinfeldt, N. In Situ Monitoring of Pt Nanoparticle Formation in Ethylene Glycol Solution by SAXS-Influence of the NaOH to Pt Ratio. *Langmuir* **2012**, *28*, 13072–13079.
- (40) Calvin, S.; Miller, M. M.; Goswami, R.; Cheng, S. F.; Mulvaney, S. P.; Whitman, L. J.; Harris, V. G. Determination of Crystallite Size in a Magnetic Nanocomposite Using Extended X-ray Absorption Fine Structure. *J. Appl. Phys.* **2003**, *94*, 778–783.
- (41) Montejano Carrizales, J. M.; Aguilera Granja, F.; Moran Lopez, J. L. Direct Enumeration of the Geometrical Characteristics of Clusters. *Nanostruct. Mater.* **1997**, *8*, 269–287.
- (42) Billinge, S. J. L.; Kanatzidis, M. G. Beyond Crystallography: the Study of Disorder, Nanocrystallinity and Crystallographically Challenged Materials with Pair Distribution Functions. *Chem. Commun.* **2004**, 749–760.
- (43) Billinge, S. J. L.; Levin, I. The Problem with Determining Atomic Structure at the Nanoscale. *Science* **2007**, *316*, 561–565.
- (44) Jensen, K. M. O.; Juhas, P.; Tofanelli, M. A.; Heinecke, C. L.; Vaughan, G.; Ackerson, C. J.; Billinge, S. J. L. Polymorphism in Magic-sized Au₁₄₄(SR)₆₀ Clusters. *Nat. Commun.* **2016**, *7*, 11859.
- (45) Leontyev, I. N.; Kuriganova, A. B.; Leontyev, N. G.; Hennes, L.; Rakhmatullin, A.; Smirnova, N. V.; Dmitriev, V. Size Dependence of the Lattice Parameters of Carbon Supported Platinum Nanoparticles: X-ray Diffraction Analysis and Theoretical Considerations. *RSC Adv.* **2014**, *4*, 35959–35965.
- (46) Zhu, F. J.; Kim, J.; Tsao, K. C.; Zhang, J. L.; Yang, H. Recent Development in the Preparation of Nanoparticles as Fuel Cell Catalysts. *Curr. Opin. Chem. Eng.* **2015**, *8*, 89–97.
- (47) Arenz, M.; Mayrhofer, K. J. J.; Stamenkovic, V.; Blizanac, B. B.; Tomoyuki, T.; Ross, P. N.; Markovic, N. M. The Effect of the Particle Size on the Kinetics of CO Electrooxidation on High Surface Area Pt Catalysts. *J. Am. Chem. Soc.* **2005**, *127*, 6819–6829.
- (48) Oh, H.-S.; Oh, J.-G.; Hong, Y.-G.; Kim, H. Investigation of carbon-supported Pt nanocatalyst preparation by the polyol process for fuel cell applications. *Electrochim. Acta* **2007**, *52* (25), 7278–7285.
- (49) Oh, H.-S.; Oh, J.-G.; Kim, H. Modification of Polyol Process for Synthesis of Highly Platinum Loaded Platinum-Carbon Catalysts for Fuel Cells. *J. Power Sources* **2008**, *183*, 600–603.
- (50) Nesselberger, M.; Ashton, S.; Meier, J. C.; Katsounaros, I.; Mayrhofer, K. J. J.; Arenz, M. The Particle Size Effect on the Oxygen Reduction Reaction Activity of Pt Catalysts: Influence of Electrolyte and Relation to Single Crystal Models. *J. Am. Chem. Soc.* **2011**, *133*, 17428–17433.
- (51) Inaba, M.; Quinson, J.; Arenz, M. pH matters: The Influence of the Catalyst Ink on the Oxygen Reduction Activity Determined in Thin Film Rotating Disk Electrode Measurements. *J. Power Sources* **2017**, *353*, 19–27.
- (52) Kacenauskaite, L.; Quinson, J.; Schultz, H.; Kirkensgaard, J. J. K.; Kunz, S.; Vosch, T.; Arenz, M. UV-Induced Synthesis and Stabilization of Surfactant-Free Colloidal Pt Nanoparticles with Controlled Particle Size in Ethylene Glycol. *ChemNanoMat* **2017**, *3*, 89–93.
- (53) Kacenauskaite, L.; Swane, A. A.; Kirkensgaard, J. J. K.; Fleige, M.; Kunz, S.; Vosch, T.; Arenz, M. Synthesis Mechanism and Influence of Light on Unprotected Platinum Nanoparticles Synthesis at Room Temperature. *ChemNanoMat* **2016**, *2*, 104–107.
- (54) Newville, M. IFEFFIT: Interactive XAFS Analysis and FEFF Fitting. *J. Synchrotron Radiat.* **2001**, *8*, 322–324.
- (55) Hammersley, A. P.; Svensson, S. O.; Hanfland, M.; Fitch, A. N.; Hausermann, D. Two-Dimensional Detector Software: From Real Detector to Idealised Image or Two-Theta Scan. *High Pressure Res.* **1996**, *14*, 235–248.
- (56) Yang, X.; Juhas, P.; Farrow, C. L.; Billinge, S. J. L. xPDFsuite: an End-to-End Software Solution for High Throughput Pair Distribution Function Transformation, Visualization and Analysis. *arXiv:1402.3163 [cond-mat.mtrl-sci]*, 2015.
- (57) Juhas, P.; Farrow, C. L.; Yang, X.; Knox, K. R.; Billinge, S. J. L. Complex Modeling: a Strategy and Software Program for Combining Multiple Information Sources to Solve Ill Posed Structure and Nanostructure Inverse Problems. *Acta Crystallogr., Sect. A: Found. Adv.* **2015**, *71*, 562–568.